TISSUE ENGINEERING: Part A
Volume 15, Number 6, 2009

DOI: 10.1089/ten.tea.2008.0134

Nanofabricated Collagen-Inspired Synthetic Elastomers for Primary Rat Hepatocyte Culture

Christopher J. Bettinger, Ph.D.,[1,2] Katherine M. Kulig, B.S.,[3] Joseph P. Vacanti, M.D.,[3] Robert Langer, Sc.D.,[4] and Jeffrey T. Borenstein, Ph.D.[2]

Synthetic substrates that mimic the properties of extracellular matrix proteins hold significant promise for use in systems designed for tissue engineering applications. In this report, we designed a synthetic polymeric substrate that is intended to mimic chemical, mechanical, and topological characteristics of collagen. We found that elastomeric poly(ester amide) substrates modified with replica-molded nanotopographic features enhanced initial attachment, spreading, and adhesion of primary rat hepatocytes. Further, hepatocytes cultured on nanotopographic substrates also demonstrated reduced albumin secretion and urea synthesis, which is indicative of strongly adherent hepatocytes. These results suggest that these engineered substrates can function as synthetic collagen analogs for *in vitro* cell culture.

Introduction

Biomaterial development has become a substantial component in tissue engineering. The primary drivers for this thrust have been the pursuit of cell–biomaterial interactions that induce appropriate interactions to promote attachment, enhance cell function, or both. Hepatic tissue engineering is of particular interest for a variety of applications, including bioartificial liver optimization, *in vitro* toxicity models,[1] and cell-based therapeutic tissue engineering devices.[2] A wide variety of natural[3] and synthetic biomaterials have been engineered and synthesized with the goal of recapitulating native hepatocyte behavior *in vitro*. Engineering natural materials has focused primarily on novel methods for production and purification of native extracellular matrix (ECM) proteins such as collagen.[4–6] ECM proteins support cell attachment and incite a variety of functions in many cells types, including hepatocytes.[3,7] However, natural ECM proteins have a limited range of properties, are subject to difficult bulk material processing, and have the potential to induce potentially dangerous immune responses when used as xenografts or allografts.[8] Natural protein extraction and purification directly from tissues also leads to significant batch-to-batch variations.[9] These variations can lead to unpredictable cell behavior, which can impact performance of cell-based tissue-engineered devices for therapeutic and drug discovery applications.[1] Synthetic peptide biomaterials produced through recombinant DNA and protein engineering strategies have been introduced as a possible means to overcome these limitations in natural peptides.[10] Although protein-based biomaterials have shown promise in achieving native-like properties through synthetic polypeptide sequences,[11] materials synthesis and production is very costly due to the dependence upon recombinant microbial hosts for synthesis and subsequent purification steps. Numerous biodegradable, synthetic thermoplastic, thermoset, and photocrosslinkable polyesters have been developed for tissue engineering applications.[12–22] Although these materials can be synthesized in large batches, most of these materials lack sufficient physicochemical properties to induce native cell function. Hence, synthetic biomaterial systems typically rely on a variety of surface treatment techniques to improve cell–biomaterial response, including protein coatings,[23] physical modification,[24] chemical modification,[25] and biotinylated conjugates to enhance adhesion.[26]

We hypothesized that an entirely synthetic biomaterial could be engineered to promote attachment and native function of primary hepatocytes, a difficult cell to culture *in vitro*.[27] The rationale behind synthesis was aimed at the biomimicry of surface chemistry and nanotopography of native collagen films. Collagen molecules are primarily composed of repeating polypeptide sequences with amide linkages.[28] Although the physical dimensions of individual molecules is 300 nm in length and 1.5 nm in width,[29] these individual molecules can form fibrils that extend for tens of microns in length and have diameters between 260 and 410 nm.[30] This

[1]Department of Materials Science and Engineering, Massachusetts Institute of Technology, Cambridge, Massachusetts.
[2]Charles Stark Draper Laboratory, Biomedical Engineering Center, Cambridge, Massachusetts.
[3]Massachusetts General Hospital, Harvard Medical School, Boston, Massachusetts.
[4]Department of Chemical Engineering, Massachusetts Institute of Technology, Cambridge, Massachusetts.

report explores the recapitulation of native nanotopography in synthetic biodegradable elastomers for use as a substrate for primary hepatocyte culture. Poly(ester amide) elastomers were chosen as a platform material because they contain chemical moieties and mechanical properties that are similar to that of native amorphous collagen fibrils. Poly(ester amide) substrates were nanofabricated to produce pillar geometries of approximately 400 nm in width to mimic the length scale of native topographical features in the synthetic polymer system. Nanotopographic poly(ester amide) substrates were found to enhance the attachment and spreading of primary hepatocytes. The morphology and metabolic function of hepatocytes cultured on nanotopographic poly(ester amides) was found to approach that of hepatocytes cultured on collagen films.

Materials and Methods

Preparation of nanofabricated silicon masters

All chemicals were acquired from Sigma (St. Louis, MO) and used as received unless otherwise stated. Photolithographic and plasma etching techniques were utilized to produce negative-mold silicon masters for use in replica molding in a similar manner to that used to produce poly (di-methylsiloxane) (PDMS).[31] Four-inch-diameter silicon wafers were oxidized for 10 h at 1100°C in atmospheric pressure oxygen at 50 standard cubic centimeters per minute flow rate (sccm), and hydrogen (30 sccm) to grow an oxide layer of 2 μm. The oxide layer thickness was measured with Filmetrics F20 and F50 spectral reflectometers. Silicon wafers with oxide layer were baked at 110°C to dehydrate their surface and spin-coated with hexamethyldisilazane (HMDS) at 5000 rpm for 10 s to promote resist adhesion. Photoresist (Shipley 1805) was then spin-coated (EVG101) on the wafers at 3500 rpm for 20 s. The wafers were then soft-baked on a hotplate at 115°C for 1 min to yield a resist film thickness of approximately 500 nm. Resist exposure was done with a Karl Suss MA-6 contact aligner with an exposure dose of 96 mJ/cm^2, and the resist was developed for 45 s in Shipley MF-319 developer followed by a 3-min rinse in deionized water and spin drying. Wafers were etched using a silicon ICP etch process using SF_6/Ar in a VLR-700 (Surface Technology Systems (STS), Newport, South Wales, UK) using etch-passivation cycles, plasma ashed, and cleaned in preparation for replica molding using photomesh patterns obtained from MEMS Exchange (Reston, VA). The remaining photoresist was stripped in a series of acetone, isopropanol, and methanol rinses. Micromachined silicon masters were cleaned using piranha solution (Mallinckrodt, St. Louis, MO) and plasma cleaned (March, St. Petersburg, FL) at 250 mT and 100 W for 120 s. Wafers were then passivated using the STS etcher with only SF_6 gas for 30 s to create a hydrophobic layer to enhance release of replica-molded substrates. Wafers were rinsed with methanol immediately before replica molding of polymers.

Replica molding of poly(ester amide) elastomers

Poly(1,3-diamino-2-hydroxypropane-*co*-polyol sebacate) (APS) prepolymers were synthesized as previously described.[32] A poly(1,3-diamino-2-hydroxypropane-*co*-gycerol sebacate) (2:1 ratio of 1,3-diamino-2-hydroxypropane: glycerol) and a poly(1,3-diamino-2-hydroxypropane-*co*-D, L-threiotol sebacate) (2:1 ratio of 1,3-diamino-2-hydroxypropane:threitol) were selected for use in hepatocyte–biomaterial interaction studies. The notation of these two elastomeric substrates was selected as 2DAHP-1G and 2DAHP-1T, respectively. This was selected to indicate the 2:1 ratio of 1,3-diamino-2-hydroxy propane (DAHP) to glycerol (G) and the 2:1 ratio of DAHP to threitol (T), respectively. The prepolymer was allowed to cool and stored at room temperature in a desiccate environment until further use. The replica molding process is shown in Figure 1. Approximately 3.5 ± 0.05 g per 20 cm^2 of APS prepolymer was melted at 170°C and applied to wafers for replica molding and smooth sheet formation. The polymer was cured at 170°C for 48 h under a vacuum of 50 mT, which produced firm, highly cross-linked, elastomeric APS polymer films of approximately 500 μm in thickness. APS polymers were statically incubated in a double distilled (ddH_2O) bath at 70°C for 24 h to induce delamination. The APS substrate was then serially placed in solutions consisting of 100% ethanol (Pharmco, Brookfield, CT) for 24 h, 70% (v/v) ethanol in ddH_2O for 2 h, 35% (v/v) ethanol in ddH_2O for 2 h, and 100% (v/v) ddH_2O for 24 h. APS polymers were dried at 70°C for 24 h and autoclaved and dried for 20 min each. The substrates were then irradiated with UV in a laminar flow hood for 15 min and incubated at 37°C for 1 h before cell seeding.

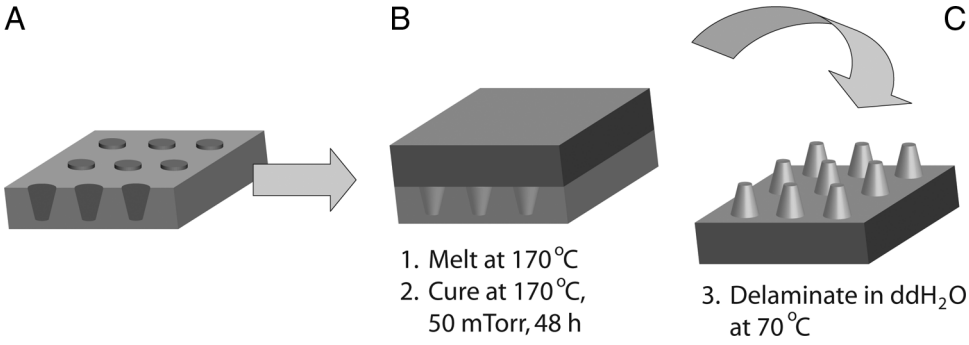

FIG. 1. Preparation of replica-molded nanofabricated APS substrates. (**A**) Passivated silicon molds are rinsed with methanol before application of the APS prepolymer. (**B**) APS prepolymers are heated to 170°C to facilitate spreading across the mold. APS polymers are then cured at 170°C under 50 mT vacuum for 48 h to induce crosslinking. (**C**) The crosslinked APS elastomers are then delaminated in ddH2O at 70°C. Note: Schematic not drawn to scale.

Preparation of collagen substrates

Collagen-coated PDMS was chosen as the control biomaterial. PDMS (Dow Sylgard 184; Essex Chemical, Clifton, NJ) was chosen as a base material due to ease of fabrication, optical clarity to facilitate characterization, and similar Young's modulus to APS polymers.[33] Briefly, substrates were plasma cleaned (PDC-001; Harrick Scientific, Pleasantville, NY) for 300 s at 80 W RF power with atmospheric gas at 250 mT. A 50 μg/mL solution of collagen I from rat tail in PBS (Sigma) was immediately adsorbed onto the surface and incubated for 2 h at 37°C.

Substrate characterization

Surface topology of nanofabricated substrates was determined using both optical microscopy and scanning electron microscopy (SEM). Hydrated and dehydrated APS substrates were imaged using optical microscopy (Nikon Imaging, Melville, NY). Dehydrated APS substrates were imaged by SEM by undergoing a dehydration bake at 70°C for 15 h followed by sputter coating with gold/palladium using a Cressington 108 Auto sputter coater for 36 s. This process deposited a 30–45-nm-thick conductive film to eliminate charging of the sample (Cressington Scientific Instruments, Cranberry Twp, PA).

Primary hepatocyte isolation and seeding

Primary rat hepatocytes were isolated using a two-step collagenase digestion as previously described.[34] Briefly, adult male Lewis rats were anesthetized, and then prepared and draped in a sterile environment. After a midline incision was made, the infrahepatic inferior vena cava was cannulated with a 16-gauge angiocath (Critikon, Tampa, FL). The suprahepatic inferior vena cava was then ligated, and the portal vein was incised to allow for retrograde efflux. Blood within the liver was washed out with an isotonic saline solution. The ECM was digested with a 0.10% type II collagenase solution (Worthington Biochemical, Lakewood, NJ). The liver was excised and mechanically agitated, resulting in a single-cell suspension. Viable hepatocytes were isolated from cellular debris and nonparenchymal liver cells by differential sedimentation at 4°C at 50 *g*. Hepatocyte number and viability were determined by trypan blue exclusion. Cells were resuspended in serum-free hepatocyte growth medium. Hepatocytes were then immediately seeded on untreated APS and collagen substrates at a density of approximately 200,000 cells/cm^2 in serum-free medium. Cells on substrates were incubated at 37°C and 5% CO_2 at 95% relative humidity. Cells were cultured in serum-free medium for the first 24 h to prevent serum proteins from interfering with cell–substrate interactions, rinsed once with DPBS, and replaced with serum-containing medium.

Characterization of cell–biomaterial response

Cell density was characterized by calculating cell density at 24, 72, 120, and 168 h time points by cell counting at 10 representative regions per well (Nikon Eclipse TE2000-U; Nikon Imaging). Initial cell attachment was calculated by normalizing cell density at 24 h with that of the cell density of the collagen substrate. Cell adhesion was calculated by assessing the relative attachment per condition at 120 h versus 24 h. Cell attachment and adhesion was calculated across three independent experiments ($n = 18$ in total). Cell morphology was characterized after 24 h by light microscopy and scanning electron microscopy. Cell areas were calculated by measuring at least 150 cells per condition across two independent experiments using AxioVision software (Zeiss Imaging, Thornwood, NY). Cell samples selected for SEM imaging were fixed using Accustain formalin-free fixative (Sigma). The samples were rinsed thrice in DPBS and immersed in solutions of 25%, 50%, 75%, and 90% (v/v) ethanol in ddH_2O for 5 min each. The samples were then immersed in 100% ethanol followed by HMDS (Sigma) each for 15 min. The samples were then allowed to air dry for 24 h before imaging. Samples were sputter-coated for 12 s, resulting in a film thickness between 10–15 nm. Scanning electron micrographs were taken using a Hitachi S-3500 N at 5 kV acceleration voltage unless otherwise noted.

Assessment of hepatocyte function

Hepatocyte function was assessed by the traditional metrics of albumin secretion and urea production ($n = 6$) across two independent experiments. For albumin secretion, medium was harvested at 24, 72, 120, and 168 h time points and stored at −20°C until further analysis. Medium was replaced with hepatocyte growth medium containing 2 μM ammonia. Cells were incubated with ammonia-containing medium for 3 h at which point the medium was harvested and stored at −20°C. Medium was then replaced with regular hepatocyte growth medium until the next time point. Albumin concentrations were measured by rat-specific albumin ELISA assay (Bethyl Laboratories, Montgomery, TX), and urea concentrations were measured by urea quantification assay (QuantiChrom; BioAssay Systems, Hayward, CA). Albumin secretion rates and urea synthesis rates were normalized by cell density.

Statistical methods

All graphical and tabulated data are displayed as mean ± SD. Significance tests to assess the effect of specific substrates for cell attachment, adherence, and spreading were conducted using an unpaired, nonparametric Kruskal–Wallis one-way ANOVA with Dunn's multiple comparison posttests (GraphPad Prism 4.0; GraphPad Software, San Diego, CA). The specific effect of nanotopography was also further analyzed by a two-tailed Student's *t*-test (Microsoft Excel, Redmond, WA). Significance tests to assess the effect of specific substrates on cell metabolism were conducted using a paired, nonparametric two-way ANOVA with Bonferroni posttests. Significance levels for all statistical methods were set at $^*p < 0.05$, $^{**}p < 0.01$, and $^{***}p < 0.001$.

Results

Nanofabricated elastomeric poly(ester amide) substrates

Silicon molds had pits of approximately 600 nm in diameter, 1200 nm in pitch, and 1000 ± 250 nm in height. The replica molding process designed for the fabrication of nanometer scale features produced substrates with high feature fidelity (Fig. 2). The column features on these substrates have approximate dimensions of 400 nm at the tip and 600 nm at the base with feature heights of 1000 nm and a

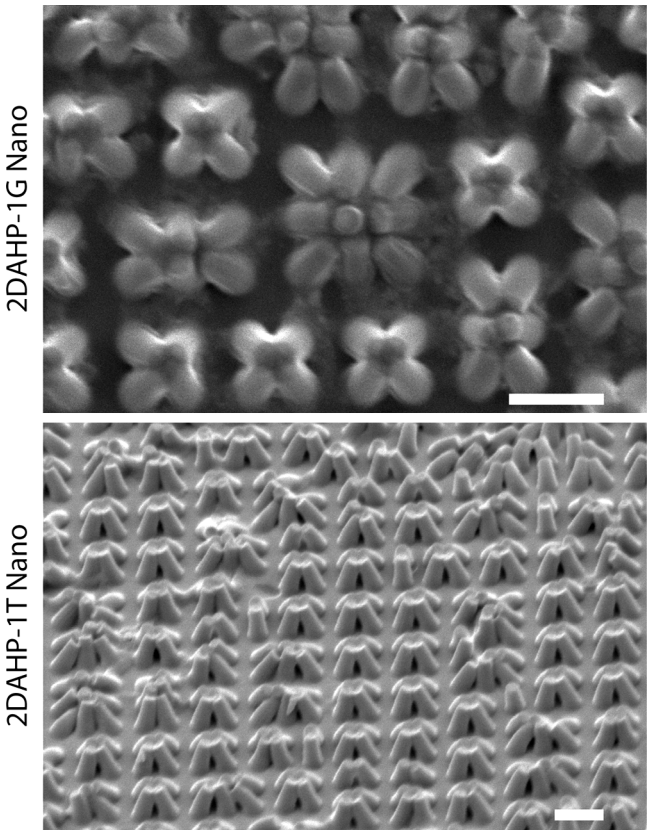

FIG. 2. Replica-molded nanofabricated APS substrates. Replica molding of both 2DAHP- 1G (0° tilt) and 2DAHP-1T (45° tilt) formulations are able to reproduce nanometer-scale features with high fidelity. The column features on these substrates have approximate dimensions of 400 nm at the tip and 600 nm at the base with feature heights of 1000 nm and a pitch of 1200 nm. Note the collapsing of these structures upon each other in the dehydrated state. The ordering of these features is restored upon hydration. Scale bars represent 2 μm.

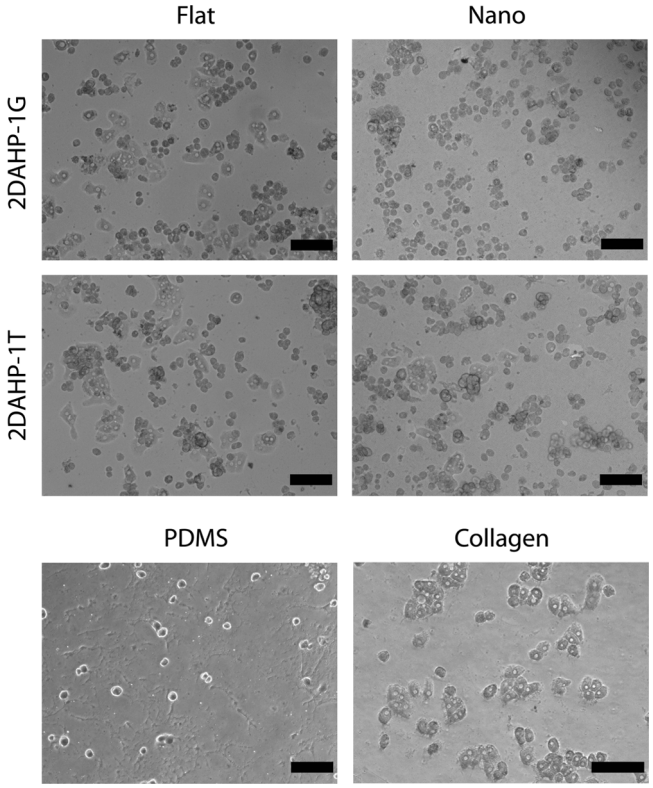

FIG. 3. Phase contrast imaging of primary rat hepatocytes on nanofabricated APS substrates. The morphology of hepatocytes seeded on uncoated APS substrates in the absence of serum for 24 h appeared similar to that of collagen substrates. However, cells cultured on collagen substrates more readily organized into multicellular structures. Hepatocytes cultured on PDMS exhibited less cell attachment and a non-native morphology. Scale bars represent 200 μm.

pitch of 1200 nm. These features appeared collapsed in the dehydrated state (Supplemental Fig. S1b, available online at www.liebertonline.com/ten), which is likely due to the combination of (1) van der Waals attraction, which is dominant on the nanometer length scale, and (2) the low mechanical modulus of APS elastomers, which cannot resist these forces. While this phenomenon has been observed in nanometer-scale features in other low-modulus substrate materials,[35,36] high-modulus materials replica molded from these substrates have been shown to resist this collapsing.[37] Further, once the substrate is hydrated, the collapsing force is relieved and the pillars are restored to an ordered formation (Supplemental Fig. S1a, available online at www.liebertonline.com/ten). This ordering of features in the hydrated condition is also confirmed by microscopy of cell-seeded substrates (Supplemental Fig. S2, available online at www.liebertonline.com/ten).

Poly(ester amide) elastomers support attachment and maintain native morphology of primary rat hepatocytes

Elastomeric poly(ester amides) supported the attachment and spreading of hepatocytes without the use of coating in serum-free conditions. The morphology of hepatocytes seeded on APS substrates was generally similar to that of hepatocytes cultured on collagen substrates (Fig. 3). The morphology of hepatocytes cultured on PDMS substrates indicated a non-native morphology and poor spreading, as expected. PDMS substrates supported the attachment of a small number of hepatocytes with limited spreading as measured by a smaller projected surface area. Hepatocyte morphology appeared to be rounded, as determined by SEM. Further, there appeared to be protrusions extending from hepatocytes cultured on nanotopographic 2DAHP-1G substrates (Fig. 4, white arrows). These cell components were also observed in hepatocytes cultured on flat 2DAHP-1T and collagen substrates (Fig. 4, white arrows).

Nanotopographic poly(ester amide) elastomers enhance attachment and spreading

Nanotopographic APS substrates were found to impact both the initial adhesion and spreading of primary hepatocytes (Fig. 5). This effect was evident on both APS elastomers. In the 2DAHP-1G formulation, the relative initial attachment was increased from approximately 0.41 ± 0.11 to 0.55 ± 0.18 ($^*p < 0.05$). A more dramatic increase was observed in the 2DAHP-1T formulation in which the relative attachment was increased from 0.51 ± 0.12 to 0.75 ± 0.22

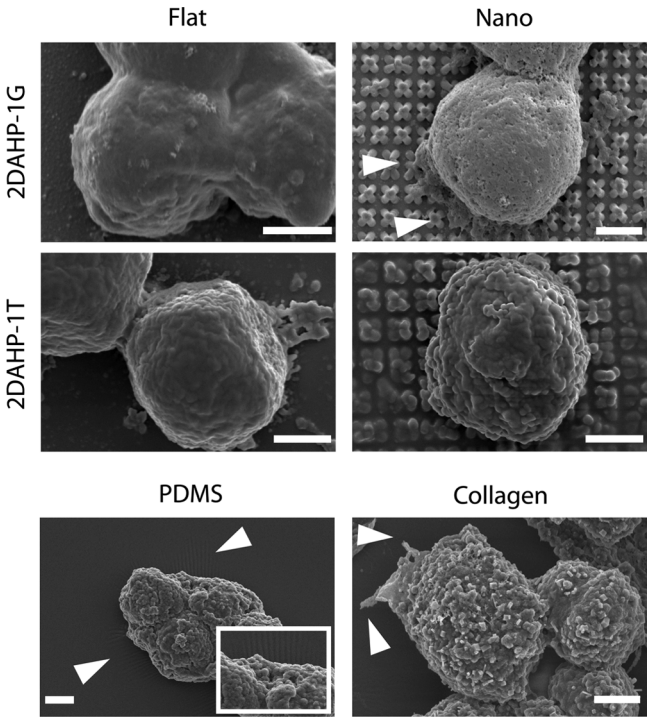

FIG. 4. Detailed morphology of cell–substrate interactions. Hepatocytes cultured on all APS substrates exhibited a rounded morphology, while those cultured on PDMS and collagen substrates exhibited a more flattened morphology. Hepatocytes appear to have extended filopodia on nanotopographic 2DAHP-1G, flat 2DAHP-1T, and collagen substrates (see white arrows). Hepatocytes induced wrinkling of PDMS substrates (see white arrows and inset). Again, note the collapsing of the posts on the nanotopographic substrates due to van der Waals forces. Scale bars represent 2 μm.

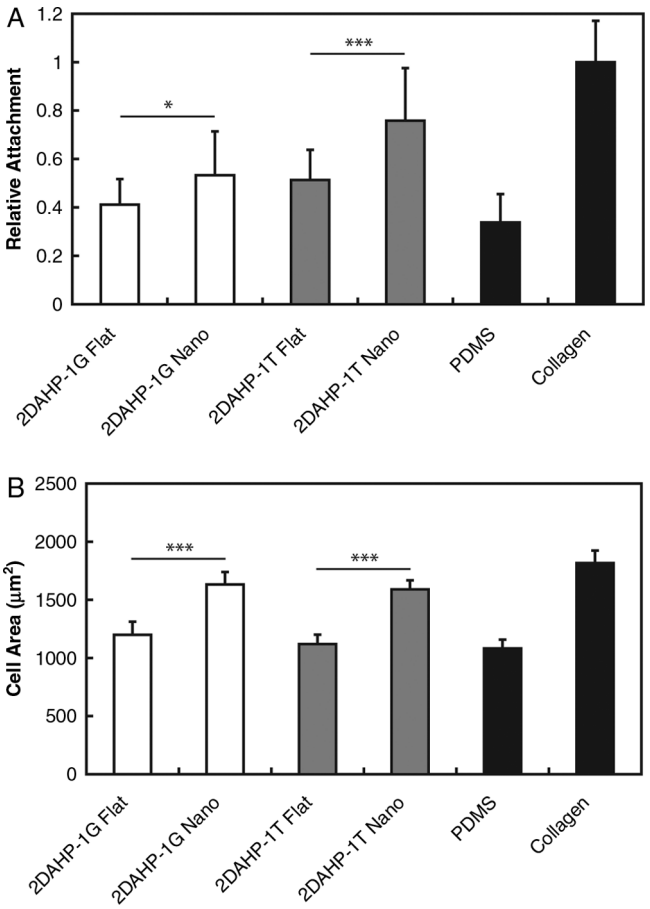

FIG. 5. Nanofabricated APS substrates improve initial attachment and increase spreading of primary hepatocytes. (**A**) Nanotopographic APS substrates increased the degree of initial hepatocyte attachment over flat APS substrate counterparts (normalized to collagen substrates). (**B**) A similar trend was found in the case of projected cell area, which serves as a metric for cell spreading. Significance levels ($*p < 0.05$ and $***p < 0.001$) determined by two-tailed Student's *t*-test. The spreading of hepatocytes cultured on flat APS substrates was significantly reduced compared to hepatocytes cultured on collagen ($***p < 0.001$ for both 2DAHP-1G and 2DAHP-1T). Further, the spreading of hepatocytes on nanotopographic APS substrates was observed to be comparable to collagen ($p > 0.05$ for both 2DAHP-1G and 2DAHP-1T).

($***p < 0.001$). Nanotopographic surfaces also enhanced the spreading of hepatocytes on APS substrates as measured by the increase in projected cell area. The cell area of hepatocytes cultured on nanotopographic APS substrates versus flat APS substrates was increased by approximately 30% across both polymers. In the case of 2DAHP-1G and 2DAHP-1T, cell area of hepatocytes was increased from 1199 ± 112 to $1633 \pm 108\,\mu m^2$ and from 1119 ± 81 to $1589 \pm 79\,\mu m^2$, respectively. The cell area of hepatocytes cultured on both flat substrates was significantly less than that of those cultured on collagen ($***p < 0.001$ for both 2DAHP-1G and 2DAHP-1T), while the cell area of hepatocytes cultured on both nanotopographic substrates was comparable to that of those cultured on collagen ($p > 0.05$). In addition to enhanced attachment and spreading, nanotopographic APS substrates also enhanced adhesion of primary hepatocytes (Fig. 6), which was determined by examining the relative cell densities after 120 h, which resulted in a series of six cumulative wash steps. Hepatocytes cultured on 2DAHP-1G Flat and 2DAHP-1T Flat substrates exhibited adhesion that was significantly less than that of those cultured on collagen substrates ($**p < 0.01$ and $***p < 0.001$, respectively), while hepatocytes cultured on both nanotopographic substrates exhibited comparable adhesion to those cultured on collagen ($p > 0.05$ for both substrates). The observed statistical similarities in spreading and adhesion between nanotopographic APS substrates and collagen substrates suggest that topography is an important component of recapitulating native ECM function *in vitro*.

Maintenance of liver function in hepatocytes cultured on poly(ester amide) elastomers

Liver-specific function of primary hepatocytes cultured on APS substrates was maintained, as assessed by albumin secretion and urea conversion (Fig. 7). The normalized albumin secretion rate is reduced significantly from day 1 to day 7 in hepatocytes cultured on all substrates. This can be attributed to the characteristic reduction of liver-specific function of hepatocytes *in vitro*. Albumin secretion was increased significantly in 2DAHP-1T Flat versus 2DAHP-1T Nano

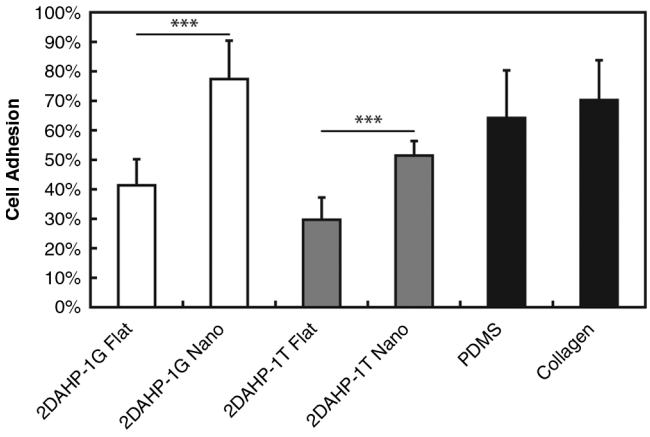

FIG. 6. Nanotopography increases the adhesion of primary hepatocytes. Nanotopographic substrates increased the relative adhesion of hepatocytes to APS substrates. The nanotopographic 2DAHP-1G formulation exhibited a higher amount of relative adhesion than collagen substrates. Significance levels (***$p < 0.001$) determined by two-tailed Student's *t*-test. Similar trends observed in spreading were also observed in the adhesion of hepatocytes, with respect to the effect of nanotopography. Namely, the adhesion of hepatocytes cultured on flat APS substrates was significantly reduced compared to hepatocytes cultured on collagen (**$p < 0.01$ for 2DAHP-1G and ***$p < 0.001$ for 2DAHP-1T). Further, the adhesion of hepatocytes on nanotopographic APS substrates was observed to be comparable to collagen ($p > 0.05$ for both 2DAHP-1G and 2DAHP-1T).

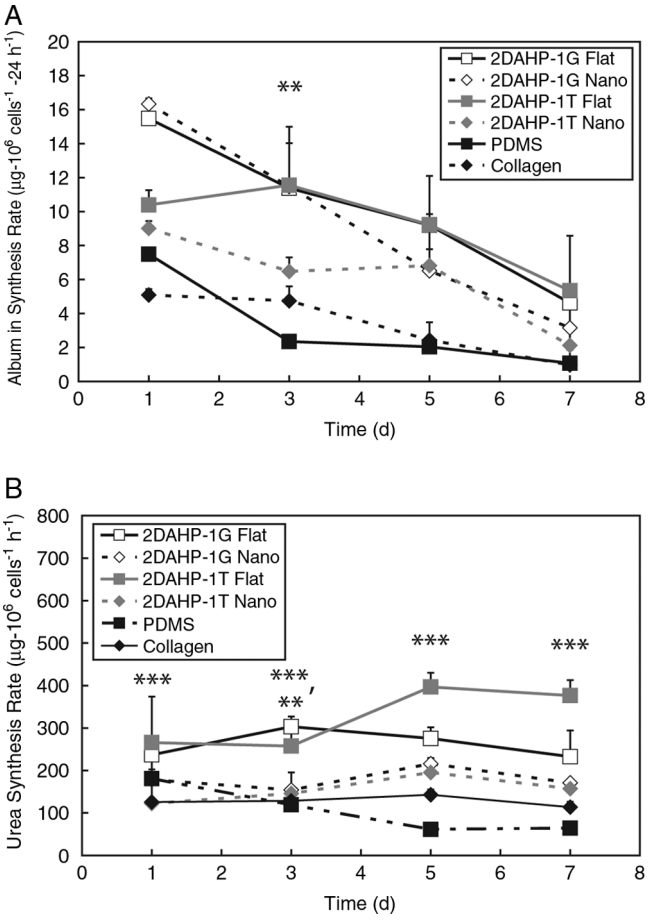

FIG. 7. Specific hepatocyte function is maintained in cells cultured on APS polymer substrates. (**A**) The normalized albumin secretion rate is reduced significantly from day 1 to day 7 in hepatocytes cultured on all substrates. This can be attributed to the characteristic reduction of liver-specific function of hepatocytes *in vitro*. Albumin secretion was increased significantly in 2DAHP-1T Flat versus 2DAHP-1T Nano substrates at day 3 (**$p < 0.01$) as determined by two-way ANOVA with Bonferroni posttests (see *Statistical methods* section). There were no significant differences between nanotopographic and flat substrates for the 2DAHP-1G elastomer. (**B**) The normalized urea synthesis rate remained relatively stable across the entirety of the experiment. Urea synthesis rates were found to be elevated in hepatocytes cultured on 2DAHP-1T Flat versus 2DAHP-1T Nano substrates (***$p < 0.001$). This differential effect was observed across all time points. A similar increase in urea synthesis was observed in hepatocytes cultured on 2DAHP-1G Flat versus 2DAHP-1G Nano substrates at day 3. However, this effect was significant at day 3 (**$p < 0.01$).

substrates at day 3 (**$p < 0.01$). There were no significant differences between nanotopographic and flat substrates for the 2DAHP-1G elastomer. In general, the normalized rate of albumin secretion was reduced with time regardless of substrate. Albumin secretion rates, while initially having a wide range of values, appeared to converge between 2 and $6\,\mu g/(10^6\ \text{cells} \cdot 24\,h)$ in hepatocytes cultured on all studied substrates. Hepatocytes cultured on 2DAHP-1G exhibited the highest initial rate of albumin secretion regardless of the topographical condition. However, by 168 h, it appeared that hepatocytes cultured on flat APS substrates had higher albumin production than those cultured on nanotopographic APS substrates, PDMS, and collagen. Urea conversion was generally higher in hepatocytes cultured on flat APS substrates across all time points. The normalized urea synthesis rate remained relatively stable across the entirety of the experiment. Urea synthesis rates were found to be elevated in hepatocytes cultured on 2DAHP-1T Flat versus 2DAHP-1T Nano substrates (***$p < 0.001$). This differential effect was observed across all time points. A similar increase in urea synthesis was observed in hepatocytes cultured on 2DAHP-1G Flat versus 2DAHP-1G Nano substrates at day 3 (**$p < 0.01$). Surprisingly, collagen substrates induced the lowest specific rate of urea conversion at 120 and 168 h.

Discussion

Synergetic effect of nanotopography on attachment, adhesion, and spreading

This work was designed to combine chemical, mechanical, and topographical components of native ECM proteins in a synthetic biodegradable polymeric substrate for use in biomedical applications. APS poly(ester amide) elastomers were chosen as a platform material because they contain amide bonds and free amines,[32] chemical moieties that are prevalent in native proteins.[28] The mechanical properties of APS elastomers, which exhibit Young's moduli ranging from approximately 1.4 to 4.3 MPa, are similar to that of amorphous collagen, which has a Young's modulus of approximately 1 MPa.[38] This polymer was enhanced with nanofabricated topographical features as another aspect to

mimic the properties of native collagen to improve cell–biomaterial interactions. Primary hepatocytes, one of the most difficult cell phenotypes to grow *in vitro*, were chosen as the model cell type to validate our nanofabricated, biomimetic polymeric substrates. It is known that the biophysical properties of substrates can drastically reduce the genotype and phenotype of hepatocytes.[39] Although the physicochemical nature of APS elastomers alone promoted favorable cell–biomaterial interactions with hepatocytes, the addition of nanometer scale topography led to enhanced attachment, spreading, and adhesion. This result has been corroborated in other cell types, including bladder smooth muscle cells[40] and corneal epithelial cells.[41] The added effect of topography enabled the robust attachment of hepatocytes to a similar degree of collagen in terms of cell retention (Fig. 5). The attachment and adhesion of a nonnegligible density of hepatocytes to PDMS was not unexpected as other systems have utilized PDMS for the culture of hepatocyte cell lines.[42] Similarly, plasma treating with oxygen has been shown to permanently reduce the water-in-air contact angle from 113° to 97°, which could leave to subsequent improvement in attachment.[43] The observed high retention of hepatocytes on these surfaces suggests that the limited numbers of cells attached to these surfaces are tightly bound. SEM micrographs indicate wrinkling at the surface, which is indicative of strong traction forces exerted by the cell on the PDMS substrate (Fig. 4). This wrinkling artifact was not observed on any other substrate, including the flat APS or collagen substrates.

Effect of nanotopography on liver-specific function of hepatocytes

While increasing adhesion is beneficial for some cell phenotypes, it is known that increasing the adhesion of hepatocytes is sometimes counter productive with respect to the effects on liver-specific function.[44] Namely, when hepatocytes adhere to substrates and are tightly bound, there is an increase in spreading and a corresponding reduction in hepatocyte function. The corresponding increase in adhesion of hepatocytes on ECM substrates[44–47] induces a reduction in liver-specific function.[48] Conversely, hepatocytes maintain liver-specific function when cultured in loosely adhered medium such as gels.[44,49–51] The results of this study corroborate with these previous studies in the context of nanotopography. Namely, the increase in hepatocyte adhesion due to nanotopography simultaneously reduces the efficiency of liver function. A similar trend is observed in the case of collagen substrates in which increased attachment, adhesion, and spreading correlate negatively with liver-specific function. In this sense, the nanofabricated synthetic APS elastomeric substrates induce hepatocyte behavior and function that trends toward that of native collagen, with respect to substrates that are physically and chemically identical, yet lack nanotopographic features.

Synthetic biomaterials that mimic the properties of native ECM molecules have a large potential for utilization in a variety of medical applications. Nanotopographic APS substrates could be used as a substrate that is able to serve as a synthetic ECM for applications, where reducing batch-to-batch variation is important. Further, this synthetic ECM can be utilized for tissue engineering applications. As previously mentioned, the use of xenografts based on natural ECM protein scaffolds or matrices can lead to serious, detrimental immune responses. Synthetic polymers that can function in a similar mode to ECM proteins could provide a material platform for scaffold fabrication, which could dramatically reduce the likelihood of a negative immune response upon implantation.

APS substrates demonstrated *in vitro* biocompatibility with primary hepatocytes by supporting attachment, adhesion, native-like morphology, and liver-specific function. APS substrates modified with replica-molded nanotopography demonstrated increased attachment, spreading, and adhesion across two polymer formulations tested. The observed increase in adhesion resulted in a corresponding reduction of liver-specific cell function. A similar trend was observed in hepatocytes cultured on collagen substrates in which increased attachment and adhesion was reciprocated by reduced albumin synthesis and urea conversion. This consistent trend observed across synthetic nanotopographic elastomeric APS substrates and collagen suggests that synthetic substrates with nanotopographic features better mimic the properties of native collagen with respect to eliciting desirable cell–biomaterial interactions.

Disclosure Statement

No competing financial interests exist.

References

1. Khetani, S.R., and Bhatia, S.N. Microscale culture of human liver cells for drug development. Nat Biotechnol **26,** 120, 2007.
2. Langer, R., and Vacanti, J.P. Tissue engineering. Science **260,** 920, 1993.
3. Flaim, C.J., Chien, S., and Bhatia, S.N. An extracellular matrix microarray for probing cellular differentiation. Nat Methods **2,** 119, 2005.
4. Chevallay, B., and Herbage, D. Collagen-based biomaterials as 3D scaffold for cell cultures: applications for tissue engineering and gene therapy. Med Biol Eng Comput **38,** 211, 2000.
5. Berglund, J.D., Nerem, R.M., and Sambanis, A. Incorporation of intact elastin scaffolds in tissue-engineered collagen-based vascular grafts. Tissue Eng **10,** 1526, 2004.
6. Altman, G.H., Diaz, F., Jakuba, C., Calabro, T., Horan, R.L., Chen, J., Lu, H., Richmond, J., and Kaplan, D.L. Silk-based biomaterials. Biomaterials **24,** 401, 2003.
7. Sofia, S., McCarthy, M.B., Gronowicz, G., and Kaplan, D.L. Functionalized silk-based biomaterials for bone formation. J Biomed Mater Res **54,** 139, 2001.
8. Hsu, S.H., Whu, S.W., Hsieh, S.C., Tsai, C.L., Chen, D.C., and Tan, T.S. Evaluation of chitosan-alginate-hyaluronate complexes modified by an RGD-containing protein as tissue-engineering scaffolds for cartilage regeneration. Artif Organs **28,** 693, 2004.
9. Eschenhagen, T., Didié, M., Münzel, F., Schubert, P., Schneiderbanger, K., and Zimmermann, W.-H. 3D engineered heart tissue for replacement therapy. Basic Res Cardiol **97 Suppl. 1,** 146, 2002.
10. Hest, J.C.M.v., and Tirrell, D.A. Protein-based materials, toward a new level of structural control. Chem Commun **19,** 1897, 2001.
11. Huang, L., McMillan, R.A., Apkarian, R.P., Pourdeyhimi, B., Conticello, V.P., and Chaikof, E.L. Generation of synthetic

elastin-mimetic small diameter fibers and fiber networks. Macromolecules **33,** 2989, 2000.
12. Amsden, B., Wang, S., and Wyss, U. Synthesis and characterization of thermoset biodegradable elastomers based on star-poly(ε-caprolactone-*co*-D,L-lactide). Biomacromolecules **5,** 1399, 2004.
13. Amsden, B.G., Tse, M.Y., Turner, N.D., Knight, D.K., and Pang, S.C. *In vivo* degradation behavior of photo-cross-linked star-poly(ε-caprolactone-*co*-D,L-lactide). Biomacromolecules **7,** 365, 2006.
14. Guan, J., Sacks, M.S., Beckman, E.J., and Wagner, W.R. Synthesis, characterization, and cytocompatibility of elastomeric, biodegradable poly(ester-urethane)ureas based on poly(caprolactone) and putrescine. J Biomed Mater Res **61,** 493, 2002.
15. Guan, J., Sacks, M.S., Beckman, E.J., and Wagner, W.R. Biodegradable poly(ether ester urethane)urea elastomers based on poly(ether ester) triblock copolymers and putrescine: synthesis, characterization and cytocompatibility. Biomaterials **25,** 85, 2004.
16. Lee, S.H., Kim, B.S., Kim, S.H., Choi, S.W., Jeong, S.I., Kwon, I.K., Kang, S.W., Nikolovski, J., Mooney, D.J., Han, Y.K., and Kim, Y.H. Elastic biodegradable poly(glycolide-co-caprolactone) scaffold for tissue engineering. J Biomed Mater Res **66A,** 29, 2003.
17. Nagata, M., Machida, T., Sakai, W., and Tsusumi, N. Synthesis, characterization, and enzymatic degradation of network aliphatic copolyesters. J Polym Sci Part A **37,** 2005, 1999.
18. Nijst, C.L.E., Bruggeman, J.P., Karp, J.M., Ferreira, L., Zumbuehl, A., Bettinger, C.J., and Langer, R. Synthesis and characterization of photocurable elastomers from poly(glycerol-co-sebacate). Biomacromolecules **8,** 3067, 2007.
19. Poirier, Y., Nawrath, C., and Somerville, C. Production of polyhydroxyalkanoates, a family of biodegradable plastics and elastomers, in bacteria and plants. Nat Biotechnol **13,** 142, 1995.
20. Sodian, R., Sperling, J.S., Martin, D.P., Egozy, A., Stock, U., Mayer, J.E., and Vacanti, J.P. Technical report: fabrication of a trileaflet heart valve scaffold from a polyhydroxyalkanoate biopolyester for use in tissue engineering. Tissue Eng **6,** 183, 2000.
21. Wang, Y., Ameer, G.A., Sheppard, B.J., and Langer, R. A tough biodegradable elastomer. Nat Biotechnol **20,** 602, 2002.
22. Yang, J., Webb, A.R., and Ameer, G.A. Novel citric acid-based biodegradable elastomers for tissue engineering. Adv Mater **16,** 511, 2004.
23. Tan, W.J., Teo, G.P., Liao, K., Leong, K.W., Mao, H.-Q., and Chan, V. Adhesion contact dynamics of primary hepatocytes on poly(ethylene terephthalate) surface. Biomaterials **26,** 891, 2005.
24. Chin, V., Collins, B.E., Sailor, M.J., and Bhatia, S.N. Compatibility of primary hepatocytes with oxidized nanoporous silicon. Adv Mater **13,** 1877, 2001.
25. Yoon, J.J., Song, S.H., Lee, D.S., and Park, T.G. Immobilization of cell adhesive RGDpeptide onto the surface of highly porous biodegradable polymer scaffolds fabricated by a gas foaming/salt leaching method. Biomaterials **25,** 5613, 2004.
26. Kojima, N., Matsuo, T., and Sakai, Y. Rapid hepatic cell attachment onto biodegradable polymer surfaces without toxicity using an avidin–biotin binding system. Biomaterials **27,** 4904, 2006.
27. Guillouzo, A. Liver cell models in *in vitro* toxicology. Environ Health Perspect **106 Suppl 2,** 511, 1998.
28. Stryer, L. Biochemistry. New York: W.H. Freeman and Co., 1996.
29. Pamula, E., de Cupere, V., Dufrene, Y.F., and Rouxhet, P.G. Nanoscale organization of adsorbed collagen: influence of substrate hydrophobicity and adsorption time. J Colloid Interf Sci **271,** 80, 2004.
30. Bozec, L., van der Heijden, G., and Horton, M. Collagen fibrils: nanoscale ropes. Biophys J **92,** 70, 2007.
31. Duffy, D.C., McDonald, J.C., Schueller, J.A., and Whitesides, G.M. Rapid prototyping of microfluidic systems in poly(dimethylsiloxane). Anal Chem **70,** 4974, 1998.
32. Bettinger, C.J., Bruggeman, J.P., Borenstein, J.T., and Langer, R. Amino alcohol-based biodegradable poly(ester amide) elastomers. Biomaterials **29,** 2315, 2008.
33. Yi, Y.W., and Liu, C. Magnetic actuation of hinged microstructures. IEEE J Microelectromech Syst **8,** 10, 1999.
34. Lee, H., Cusick, R.A., Utsunomiya, H., Ma, P.X., Langer, R., and Vacanti, J.P. Effect of implantation site on hepatocytes heterotopically transplanted on biodegradable polymer scaffolds. Tissue Eng **9,** 1227, 2003.
35. Geim, A.K., Dubonos, S.V., Grogproeva, I.V., Novoselov, K.S., Zhukov, A.A., and Shapoval, S.Y. Microfabricated adhesive mimicking gecko foot-hair. Nat Mater **2,** 461, 2003.
36. Mahdavi, A., Ferreira, L., Sundback, C., Nichol, J.W., Chan, E.P., Carter, D.J.D., Bettinger, C.J., Patanavanich, S., Chignozha, L., Ben-Joseph, E., Galakatos, A., Pryor, H., Pomerantseva, I., Masiakos, P.T., Faquin, W., Zumbuehl, A., Hong, S., Borenstein, J., Vacanti, J., Langer, R., and Karp, J.M. A biodegradable and biocompatible gecko-inspired tissue adhesive. Proc Nat Acad Sci USA **105,** 2307, 2008.
37. Bettinger, C.J., Cyr, K.M., Matsumoto, A., Langer, R., Borenstein, J.T., and Kaplan, D.L. Silk fibroin microfluidic devices. Adv Mater **19,** 2847, 2007.
38. Fung, Y.C. Biomechanics: Mechanical Properties of Living Tissues. New York: Springer, 1993.
39. Lindblad, W.J., Schuetz, E.G., Redford, K.S., and Guzelian, P.S. Hepatocellular phenotype *in vitro* is influenced by biophysical features of the collagenous substratum. Hepatology **13,** 282, 1991.
40. Thapa, A., Webster, T.J., and Haberstroh, K.M. Polymers with nano-dimensional surface features enhance bladder smooth muscle cell adhesion. **67A,** 1374, 2003.
41. Karuri, N.W., Liliensiek, S., Teixeira, A.I., Abrams, G., Campbell, S., Nealey, P.F., and Murphy, C.J. Biological length scale topography enhances cell-substratum adhesion of human corneal epithelial cells. J Cell Sci **117,** 3153, 2004.
42. Leclerc, E., Yasuyuki, S., and Fujii, T. Cell culture in 3-dimensional microfluidic structure of PDMS (polydimethylsiloxane). Biomed Microdevices **5,** 109, 2003.
43. Gillmor, S.D., Larson, B.J., Braun, J.M., Mason, C.E., Cruz-Barba, L.E., Denes, F., and Lagally, M.G. Low-Contact Angle Polydimethylsiloxane (PDMS) Membranes for Fabricating Micro-Bioarrays. IEEE-EMBS Microtechnologies in Medicine and Biology. Madison, WI: IEEE, 2002, pp. 51–56.
44. Ze'ev, B., Robinson, G.S., Bucher, N.L., and Farmer, S.R. Cell-cell and cell-matrix interactions differentially regulate the expression of hepatic and cytoskeletal genes in primary cultures of rat hepatocytes. Proc Natl Acad Sci USA **85,** 2161, 1988.
45. Mooney, D., Hansen, L., Vacanti, J., Langer, R., Farmer, S., and Ingber, D. Switching from differentiation to growth in

hepatocytes: control by extracellular matrix. J Cell Physiol **151,** 497, 1992.
46. Sanchez, A., Alvarez, A.M., Pagan, R., Roncero, C., Vilaro, S., Benito, M., and Fabregat, I. Fibronectin regulates morphology, cell organization and gene expression of rat fetal hepatocytes in primary culture. J Hepatol **32,** 242, 2000.
47. Carlisle, E.S., Mariappan, M.R., Nelson, K.D., Thomes, B.E., Timmons, R.B., Constantinescu, A., Eberhart, R.C., and Bankey, P.E. Enhancing hepatocyte adhesion by pulsed plasma deposition and polyethylene glycol coupling. Tissue Eng **6,** 45, 2000.
48. Hodgkinson, C.P., Wright, M.C., and Paine, A.J. Fibronectin-mediated hepatocyte shape change reprograms cytochrome P450 2C11 gene expression via an integrin-signaled induction of ribonuclease activity. Mol Pharmacol **58,** 976, 2000.
49. Schuetz, E.G., Li, D., Omiecinski, C.J., Muller-Eberhard, U., Kleinman, H.K., Elswick, B., and Guzelian, P.S. Regulation of gene expression in adult rat hepatocytes cultured on a basement membrane matrix. J Cell Physiol **134,** 309, 1988.
50. Dunn, J.C., Yarmush, M.L., Koebe, H.G., and Tompkins, R.G. Hepatocyte function and extracellular matrix geometry: long-term culture in a sandwich configuration. FASEB J **3,** 174, 1989.
51. Hamilton, G.A., Jolley, S.L., Gilbert, D., Coon, D.J., Barros, S., and Le-Cluyse, E.L. Regulation of cell morphology and cytochrome P450 expression in human hepatocytes by extracellular matrix and cell-cell interactions. Cell Tissue Res **306,** 85, 2001.

Address reprint requests to:
Robert Langer, Sc.D.
Department of Chemical Engineering
Massachusetts Institute of Technology
77 Massachusetts Ave., Room E25-342
Cambridge, MA 02139

E-mail: rlanger@mit.edu

Jeffrey T. Borenstein, Ph.D.
Charles Stark Draper Laboratory
Biomedical Engineering Center
555 Technology Square
Cambridge, MA 02139

E-mail: jborenstein@draper.com

Received: February 29, 2008
Accepted: August 26, 2008
Online Publication Date: October 8, 2008